Applied Thermal Engineering 145 (2018) 287–294

Contents lists available at ScienceDirect

Applied Thermal Engineering

journal homepage: www.elsevier.com/locate/apthermeng

Research Paper

Measurements and modeling to determine the critical temperature for preventing thermal runaway in Li-ion cells

Iretomiwa Esho[1], Krishna Shah[1], Ankur Jain*

Mechanical and Aerospace Engineering Department, University of Texas at Arlington, Arlington, TX, USA

HIGHLIGHTS

- Develops a new method to predict the peak temperature for safety of a Li-ion cell.
- Contributes towards enhanced safety in transportation and storage of Li-ion cells.
- Quantifies trade-offs between internal and external heat transfer in Li-ion cell.
- Contributes towards prediction and prevention of thermal runaway.

ARTICLE INFO

Keywords:
Lithium ion battery
Battery safety
Thermal runaway
Battery cooling
Heat transfer

ABSTRACT

Li-ion cells are widely used for electrochemical energy conversion and storage, but suffer from safety problems due to overheating. At elevated temperatures, the cell enters a state of thermal runaway involving multiple heat-generating decomposition reactions that eventually lead to fire and explosion. Understanding the nature of thermal runaway, specifically the highest temperature that a cell can safely withstand, is critical for improving cell safety. This paper presents an experimentally validated method to predict the critical temperature based on the thermal balance between temperature-dependent heat generation, thermal conduction in the cell and heat dissipation on the cell surface. It is shown that for a single reaction case, the critical temperature can be determined from the root of a non-linear, transcendental equation involving parameters that characterize these processes. A computational model for a more realistic but complicated case of multiple reactions with reactant consumption is also presented. The predicted critical temperature is found to be in good agreement with experimental measurements on a thermal test cell in a wide range of thermal parameters. Trade-offs between cell thermal conductivity and convective heat transfer coefficient are shown to dramatically influence the critical temperature. Results presented here enable accurate prediction of the critical temperature of a Li-ion cell in a given thermal environment, and therefore, may contribute towards improved safety in the storage, transportation and operation of Li-ion cells.

1. Introduction

Li-ion batteries have been used extensively for electrochemical energy conversion and storage in electric vehicles, grid storage, consumer electronics, etc. due to superior performance characteristics compared to other technologies [1–3]. Despite these advantages, however, the adoption of Li-ion cell technology has been impeded by several safety related concerns related to overheating during operation [4,5]. In addition to safety, overheating also affects system performance, as cell and battery loads need to be designed conservatively in order to minimize the risk of thermal runaway. Thermal runaway occurs when the cell temperature exceeds a certain threshold due to insufficient rate of removal of heat generated during operation, which triggers a series of exothermic decomposition reactions and processes within a Li-ion cell including decomposition of the solid electrolyte interface (SEI) [6], decomposition of electrodes [7] and eventually, combustion of electrolyte [8]. As cell temperature rises, heat generated from such processes increases even further, which may lead to an unsustainable thermal state of the cell [9–12]. If the amount of heat generated is a strong, non-linear function of temperature that cannot be effectively dissipated out of the cell, then it results in uncontrolled temperature rise, eventually causing fire and explosion.

* Corresponding author at: 500 W First St, Rm 211, Arlington, TX 76019, USA.
E-mail address: jaina@uta.edu (A. Jain).
[1] Equal contributors.

https://doi.org/10.1016/j.applthermaleng.2018.09.016
Received 18 May 2018; Received in revised form 11 August 2018; Accepted 3 September 2018
Available online 07 September 2018
1359-4311/

Thermal runaway has been widely studied through experimental measurement and visualization. Thermal runaway is typically induced by stressing the cell through thermal, mechanical or electrical means. For example, cells have been subjected to high ambient temperature in oven tests to study the thermal threshold of thermal runaway [13–15]. Short circuit tests [16–18] have been carried out to induce large internal heating within a cell. Mechanical abuse in the form of nail penetration into a cell has also been studied extensively [19,20].

A key question of much practical relevance that several such experiments attempt to address is the maximum temperature that a Li-ion cell is capable of withstanding without entering thermal runaway. Fundamentally, thermal runaway characteristics of a cell are determined by the interactions of three distinct thermal processes [9] – heat generation within the cell due to the exothermic decomposition reactions, heat conduction within the cell, and heat dissipation from the cell surface to the surroundings. Each of these aspects has been studied in detail in the past. Heat generation is known to occur due to multiple decomposition reactions that occur simultaneously [10,11]. Arrhenius reaction parameters associated with these reactions have been measured [10,21,22]. Thermal conductivity of a Li-ion cell [23,24], as well as its material components [25–27] has been measured. Thermal contact resistance at the separator-cathode interface has been shown to dominate thermal conduction resistance within the cell [28]. Heat dissipation from the cell to the surroundings has also been investigated in detail, using a variety of methods including air cooling, liquid cooling, phase change based cooling, the use of heat pipes and thermally enhanced casing material [29–37].

While most of the past work focuses on only one of the three thermal processes behind thermal runaway, the interaction between these processes has been studied only to a limited extent. It has been shown through steady-state [38] and transient analyses [9] that the values of certain non-dimensional numbers govern whether thermal runaway occurs or not. These numbers combine the characteristics of heat generation in the form of Arrhenius parameters, thermal conduction in the form of thermal conductivity, and heat dissipation in the form of the Biot number that governs the convective conditions on the surface of the cell. Due to the complex, highly coupled nature of thermal runaway, it is important to infer from these theoretical insights, practical design guidelines that will help prevent thermal runaway. Specifically, the maximum threshold temperature, $T_{critical}$ that the cell can experience without entering thermal runaway is an important parameter not only for safety, but also for performance, as knowing the limits of thermal runaway will help make informed decisions about pushing the cell discharge load to the maximum possible without entering thermal runaway. So far, a few studies have attempted to determine the value of $T_{critical}$ through experiments in which a Li-ion cell is externally heated or exposed to different temperatures in an oven [14,15]. Strategies to prevent or limit damage caused by thermal runaway have also been studied [39,40]. Determining the value of $T_{critical}$ through theoretical insights into thermal runaway [9,38] is expected to help improve the accuracy of $T_{critical}$ measured from experiments as well as make the prevention strategies more effective. This will also provide practical guidelines for designers of Li-ion cell based energy conversion and storage systems.

This paper improves upon the present state-of-the-art by deriving the value of $T_{critical}$, the peak temperature a Li-ion cell can withstand without entering thermal runaway, as a function of various parameters based on recently-reported analysis of a non-dimensional number that governs the occurrence of thermal runaway [9]. It is shown that for the case of a single decomposition reaction, $T_{critical}$ can be determined from the root of a non-linear, transcendental equation involving characteristic parameters from heat generation, thermal conduction and convection on the cell surface. A numerical model for a more realistic and complicated condition with multiple reactions is also presented. Experimental measurements of $T_{critical}$ on a thermal test cell in a wide range of Arrhenius heat generation parameters are found to be in good agreement with theoretical predictions. Experiments that expose the thermal test cell to elevated temperature in an external oven clearly show the cell entering thermal runaway when the oven temperature is greater than the predicted value of $T_{critical}$, and heating up but not entering thermal runaway when the oven temperature is lower than $T_{critical}$. A key novelty of this work is that it results in the limits of thermal design parameters related to thermal conduction and convection towards preventing thermal runaway. These experimentally validated results provide key insight into the nature of thermal runaway not available from past work. Based on the present work, practical design and run-time control tools can be developed for ensuring maximum possible performance output without entering thermal runaway.

2. Mathematical modeling

A recent paper [9] shows that the occurrence of thermal runaway in a Li-ion cell undergoing temperature-dependent heat generation can be predicted by tracking the value of a specific non-dimensional number, referred to as the Thermal Runaway Number (*TRN*). By considering the boundedness of the solution of the transient governing energy equation with temperature-dependent heat generation rate expressed as a Taylor series expansion, it has been shown that thermal runaway occurs when the value of *TRN* exceeds 1. Mathematically, for a cylindrical cell, this threshold condition is given by [9]

$$\frac{\beta R^2}{k\mu_1^2} - 1 = 0 \tag{1}$$

where β is the slope of heat generation rate Q with respect to temperature, k is the cell radial thermal conductivity, R is the cell radius and μ_1 refers to the first root of the eigenfunction corresponding to the convective boundary condition at the outer surface of the cell [9]

$$Bi \cdot J_0(\mu_n) - \mu_n J_1(\mu_n) = 0 \tag{2}$$

Here, $Bi = \frac{h \cdot R}{k}$ refers to the Biot number, which represents the extent of convective heat transfer on the outer surface of the cell [41,42]. J_0 and J_1 refer to Bessel functions of the first kind and order 0 and 1 respectively.

In this paper, the *TRN* concept is used to examine the thermal conditions that will result in unbounded temperature, and derive a limiting condition. The critical temperature $T_{critical}$ is determined in the next two sub-sections for two distinct cases – a single reaction and multiple reactions with reactant consumption over time.

2.1. Single reaction model

A single reaction case is first considered, which is assumed to be governed by Arrhenius reaction kinetics, as is usually the case with exothermic decomposition reactions in a Li-ion cell [11]. Heat generation rate in this case is given by

$$Q(T) = Q_0 e^{\left(-\frac{E_a}{R_u T}\right)} \tag{3}$$

where Q_0 and E_a are the pre-exponential coefficient and activation energy respectively. R_u refers to the universal gas constant.

An expression for β can therefore be derived from Eq. (3) by differentiating with respect to temperature, resulting in

$$\beta(T) = \frac{dQ(T)}{dT} = Q_0 \frac{E_a}{R_u T^2} e^{\left(-\frac{E_a}{R_u T}\right)} \tag{4}$$

Eq. (4) shows that β increases with temperature, and therefore the Thermal Runaway Number increases as well. Inserting Eq. (4) in Eq. (1) results in a threshold condition for thermal runaway in terms of the cell temperature as follows:

$$\frac{Q_0 R^2 E_a}{k\mu_1^2 R_u T_{critical}^2} e^{\left(-\frac{E_a}{R_u T_{critical}}\right)} - 1 = 0 \tag{5}$$

Eq. (5) is a non-linear transcendental equation in $T_{critical}$ that does not appear to have a closed-form solution. Nevertheless, given the values of various heat generation and heat transfer parameters in Eq. (5), it can be solved numerically using a variety of methods such as the Newton Raphson method [43] to determine the value of $T_{critical}$. This provides a useful method for determining the critical temperature to prevent thermal runaway in a given set of heat generation and heat dissipation conditions. The value of $T_{critical}$ represents the maximum temperature at which the thermal balance between heat generation and heat removal processes results in a bounded temperature at large times. Beyond this value, the cell can not withstand the rate of increase of heat generation with temperature, leading to thermal runaway. It is possible that thermal runaway could be avoided if the cell spends only a very short amount of time at $T_{critical}$, however, for conservative design, and due to the critical importance of avoiding thermal runaway, $T_{critical}$ may be interpreted as the upper limit for the cell temperature.

2.2. Multiple reaction model

Thermal runaway in a Li-ion cell is known to be caused by a cascade of multiple reactions, each with distinct Arrhenius parameters [10,11]. Moreover, reactant consumption over time is an important factor that influence heat generation rate. As a result, it is helpful to extend the single reaction model presented in Section 2.1 to account for these complex processes in a Li-ion cell. In order to do so, a multiple reaction model with reactant consumption is developed. The four well-known decomposition reactions in a Li-ion cell include Solid-Electrolyte Interface (SEI) decomposition, negative electrode-solvent reaction, positive electrode-solvent reaction and electrolyte decomposition [11]. Accordingly, the net heat generation rate is given by [11]

$$Q_{exothermic} = W_c H_{sei} c_{sei} A_{sei} e^{\left(-\frac{E_{a_{sei}}}{R_u T}\right)} + W_c H_{ne} c_{ne} e^{\left(-\frac{t_{sei}}{t_{0sei}}\right)} A_{ne} e^{\left(-\frac{E_{a_{ne}}}{R_u T}\right)} + W_{pe} H_{pe} \alpha_{pe} (1-\alpha_{pe}) A_{pe} e^{\left(-\frac{E_{a_{pe}}}{R_u T}\right)} + W_e H_e c_e A_e e^{\left(-\frac{E_{a_e}}{R_u T}\right)} \quad (6)$$

Here, H, A, E_a and c are reaction heat, frequency factor, activation energy and reactant concentration respectively. Subscripts denote the corresponding reaction for each term. W is the amount of active content involved in a particular reaction while the subscript denotes the material. t_{SEI} denotes SEI thickness and α_{PE} is the conversion factor. Once these reactions initiate, heat generation rate initially increases, and then slows down due to gradual consumption of reactants. The rate of change of reactant concentration is given [11]

$$\frac{dc_{sei}}{dt} = -c_{sei} A_{sei} e^{\left(-\frac{E_{a_{sei}}}{R_u T}\right)} \quad (7)$$

$$\frac{dc_{ne}}{dt} = -c_{ne} e^{\left(-\frac{t_{sei}}{t_{0sei}}\right)} A_{ne} e^{\left(-\frac{E_{a_{ne}}}{R_u T}\right)} \quad (8)$$

$$\frac{dt_{sei}}{dt} = c_{ne} e^{\left(-\frac{t_{sei}}{t_{0sei}}\right)} A_{ne} e^{\left(-\frac{E_{a_{ne}}}{R_u T}\right)} \quad (9)$$

$$\frac{d\alpha_{pe}}{dt} = \alpha_{pe} (1-\alpha_{pe}) A_{pe} e^{\left(-\frac{E_{a_{pe}}}{R_u T}\right)} \quad (10)$$

$$\frac{dc_e}{dt} = -c_e A_e e^{\left(-\frac{E_{a_e}}{R_u T}\right)} \quad (11)$$

Initial values for these non-dimensional quantities can be found in the literature [11].

In order to develop a model for $T_{critcal}$ accounting for multiple reactions and reactant consumption, an expression for β may be written as

$$\beta(T) = \frac{dQ_{exothermic}(T)}{dT} = W_c H_{sei} A_{sei} c_{sei} \frac{E_{a_{sei}}}{R_u T^2} e^{\left(-\frac{E_{a_{sei}}}{R_u T}\right)} + W_c H_{ne} A_{ne} c_{ne} e^{\left(-\frac{t_{sei}}{t_{0sei}}\right)} \frac{E_{a_{ne}}}{R_u T^2} e^{\left(-\frac{E_{a_{ne}}}{R_u T}\right)} + W_{pe} H_{pe} A_{pe} \alpha_{pe} (1-\alpha_{pe}) \frac{E_{a_{pe}}}{R_u T^2} e^{\left(-\frac{E_{a_{pe}}}{R_u T}\right)} + W_e H_e A_e c_e \frac{E_{a_e}}{R_u T^2} e^{\left(-\frac{E_{a_e}}{R_u T}\right)} \quad (12)$$

where the concentration terms themselves change with time.

Due to the significantly increased complexity in $\beta(T)$ compared to the single reaction case, derivation of a single transcendental equation in $T_{critical}$ is not possible. Instead, a numerical approach is adopted, wherein temperature is raised with steps of ΔT, starting from room temperature, T_0, until the value of *TRN* exceeds 1. Here, *TRN* is calculated by substituting for $\beta(T)$ as given by Eq. (12) into Eq. (1). As temperature increases, reactants are consumed, and therefore the concentration terms and the value of β must both be re-computed. The rate of change of concentration with time is computed using Eqs. (7)–(11) and the rate of change of temperature with time, dT/dt is computed using a lumped mass assumption as follows:

$$\frac{dT}{dt} = \frac{(Q_{exothermic} + Q_{nominal})V + hA(T-T_\infty)}{\rho C_p V} \quad (13)$$

where $Q_{nominal}$ is the sum of ohmic, overpotential and entropic heat [10] and V is the cell volume. For a typical oven test where the cell itself is electrically inactive and is heated only by convective heat transfer from a hot oven, $Q_{nominal}$ can be considered to be zero.

The initial values of various reactant concentrations are taken from literature [11]. The value of *TRN* is therefore computed as one marches forward in temperature, and the critical temperature is taken to be that value at which *TRN* first exceeds a value of 1. It is possible that *TRN* may rise above the critical value of 1 and then come down at higher temperature due to reactant consumption. However, for conservative design, the temperature at which *TRN* first exceeds 1 is taken to be the critical temperature.

Note that this model does not account for a variety of safety features that have been implemented to prevent or delay thermal runaway, such as a shutdown separator in which a component melts and fills the separator pores, thereby stopping ion transport.

In summary, the theoretical models presented in this section predict the critical temperature in a variety of conditions, taking into account the nature of heat generation within the cell, as well as the nature of thermal transport within and outside the cell. The next section describes experiments carried out to validate the theoretical model for $T_{critical}$ presented in this section. A discussion of key results, including comparison of models with experiments and discussion of model results is presented in Section 4.

3. Experiments

A thermal test cell with the geometry of a 26650 Li-ion cell is used in this work to experimentally determine the value of $T_{critical}$ in a variety of conditions and compare against predictions from the theoretical model presented in Section 2. This thermal test cell, described in past papers [9,44,45], comprises a sheet of thin metal foil with Kapton tape insulation and embedded T-type thermocouples that is rolled into a cylinder and inserted inside the metal casing of a 26650 cell. By producing heat through Joule heating instead of electrochemically as in a 26650 Li-ion cell, the thermal test cell provides a capability of imposing and accurately measuring any desired heat generation rate, which can also be varied as a function of temperature by varying the heating current in response to the cell temperature measured by the embedded thermocouple. The thermal conductivity of the thermal test cell has been measured to be similar to that of an actual Li-ion cell (0.20 W/m K vs. 0.15 W/m K), indicating that its thermal response is expected to be

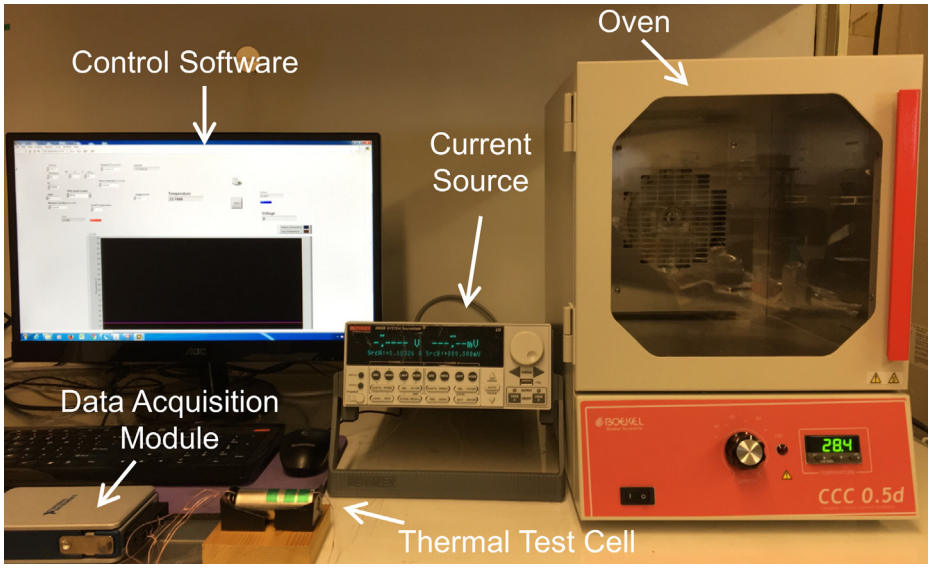

Fig. 1. Picture of the experimental setup.

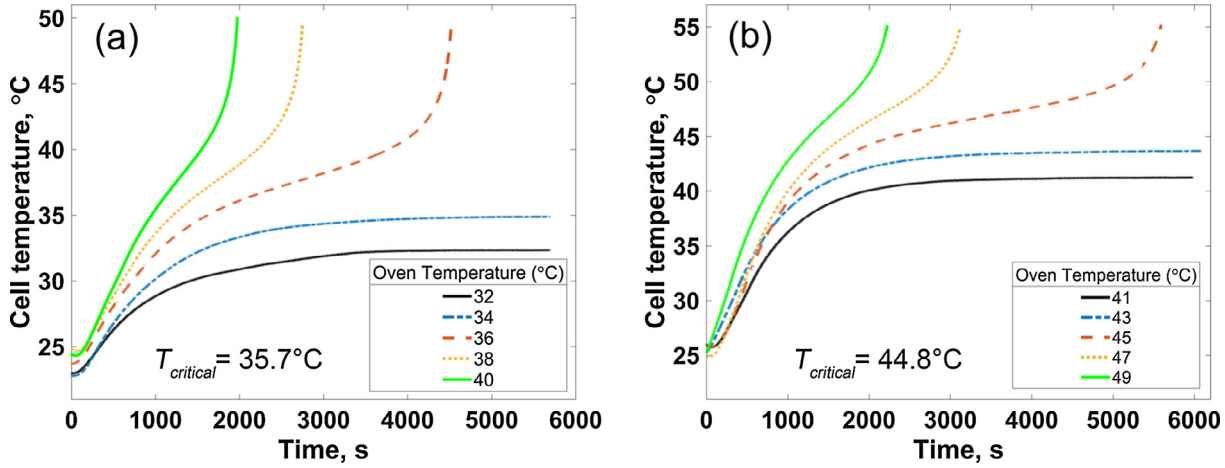

Fig. 2. Experimental measurement of cell temperature as a function of time for multiple oven temperatures when the theoretically predicted value of $T_{critical}$ is (a) 35.7 °C, and (b) 44.8 °C. In each case, thermal runaway is found to occur when the oven temperature exceeds the theoretically predicted value of $T_{critical}$.

close to that of an actual Li-ion cell. This thermal test cell has been used in a variety of recently reported measurements of thermal phenomena in Li-ion cells [9,44–46].

Temperature of the embedded thermocouple in the thermal test cell is measured through a National Instruments cDAQ-9171, connected to LabView software running on a 64-bit computer. Based on the temperature measured each second, the software updates the heating current sourced from a Keithley 2602B sourcemeter to be passed through the resistive heater in the thermal test cell. Therefore, as the cell temperature rises, so does the heat generation rate, in accordance with the desired Arrhenius relationship, parameters for which are provided as input to LabView. In this manner, the thermal test cell is capable of being heated up according to any desired, temperature-dependent heat generation rate.

Fig. 1 shows a picture of the experimental setup. A BOEKEL thermal oven is used for subjecting the thermal test cell undergoing temperature-dependent heat generation to a variety of external temperatures. The oven size is 0.02 m^3, and provides temperature stability and uniformity of ± 0.5 °C and ± 0.7 °C respectively. A T type thermocouple is placed in the oven near the thermal test cell to directly measure the ambient temperature. Experiments are carried out at multiple ambient temperatures. In each case, when the oven temperature is changed, sufficient time is provided for the oven to reach a steady-state before starting experiments. In each experiment, cell temperature is measured as a function of time to determine whether the cell enters thermal runaway or reaches a steady-state. The value of $T_{critical}$ determined in this manner is compared with predictions from the theoretical model presented in Section 2 in a variety of experimental conditions, specifically for different values of Q_0 and E_a.

4. Results and discussion

Two set of experiments are carried out, in which the Arrhenius parameters Q_0 and E_a are chosen such that the theoretically predicted value of $T_{critical}$ from Eq. (5) is 35.7 °C and 44.8 °C respectively. These numbers are chosen to be lower than the usual thermal runaway threshold temperatures in order to safely carry out these experiments in the thermal test cell. For each case of $T_{critical}$, the corresponding value of Q_0 and E_a are inserted in the LabView software, which ensures that heat generation in the test cell follows the corresponding Arrhenius kinetics. A number of experiments are then carried out in which the thermal test cell is placed in an oven set at progressively increasing temperatures. In order to validate the theoretical model for $T_{critical}$ presented in Section 2, cell temperature is measured as a function of time for a number of oven temperatures, and the value of oven temperature that results in thermal runaway is determined. These data are summarized in Fig. 2(a) and (b)

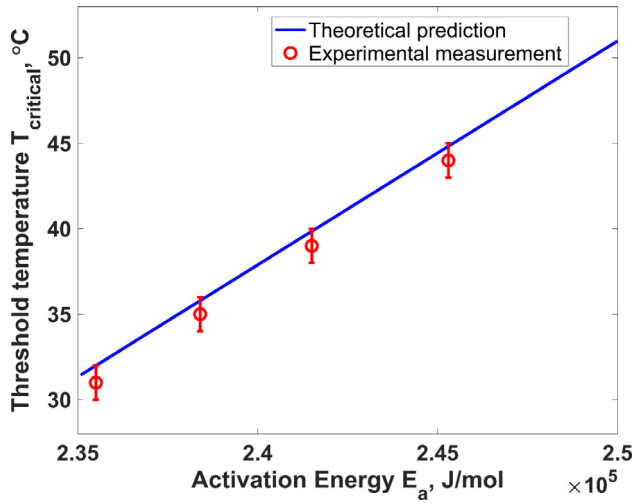

Fig. 3. Experimentally measured $T_{critical}$ for a number of values of E_a while holding Q_0 constant. Experimental data are represented by symbols, and the theoretical curve from Eq. (5) is shown for comparison.

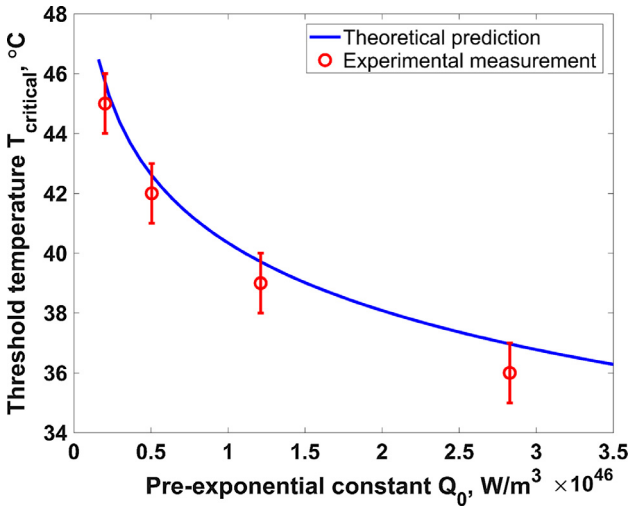

Fig. 4. Experimentally measured $T_{critical}$ for a number of values of Q_0 while holding E_a constant. Experimental data are represented by symbols, and the theoretical curve from Eq. (5) is shown for comparison.

for the two sets of experiments. Both figures show that when the oven temperature is lower than the value of $T_{critical}$, the cell temperature always reaches a steady state. In experiments where the oven temperature exceeds the value of $T_{critical}$, on the other end, the cell temperature begins to increase in an uncontrolled fashion, indicating the onset of thermal runaway. The critical temperature for inducing thermal runaway determined in both sets of these experiments matches well with the value of $T_{critical}$ for the experimental conditions. This provides an experimental validation of the theoretical model for $T_{critical}$ presented in Section 2. Even though validation of the theoretical model is shown for $T_{critical}$ values lower than is usual in actual thermal runaway in Li-ion cells, this is a reasonable approach since the experiments are designed to follow the same Arrhenius kinetics that thermal runaway is known to follow. A model that is accurate at low values of $T_{critical}$ can reasonably be expected to be accurate at relatively larger values as well, as long as the Arrhenius nature of heat generation is preserved.

For further validation of the theoretical model, a number of experiments are carried out in which the Arrhenius parameters are varied, and the theoretical model is compared against experimentally determined values of $T_{critical}$. Fig. 3 plots the experimental values of $T_{critical}$ for a number of values of activation energy E_a, while Q_0 is held constant at 10^{44} W/m^3. The theoretical curve based on the solution of equation (5) is also plotted. In each case, the theoretical model and experimental measurements are in agreement within the uncertainty range of experimental measurements. Similarly, when Q_0 is varied while holding E_a constant at 2.54×10^5 J/mol, the measured critical temperature agrees very well with the theoretical model, as shown in Fig. 4. The deviation between the two is likely due to various experimental error sources such as oven temperature measurement resolution, etc. In general, $T_{critical}$ increases when Q_0 goes down or E_a goes up. In both cases, the theoretical model is found to be capable of predicting $T_{critical}$ correctly. Figs. 2–4 provide comprehensive experimental validation of the theoretical model to predict $T_{critical}$.

The theoretical model is then used to investigate thermal runaway with multiple reactions and reactant consumption. First, $T_{critical}$ is determined as a function of activation energy corresponding to SEI reaction ($E_{a_{sei}}$), keeping all other parameters constant. SEI reaction occurs in the early stages of thermal runaway [10,11,21] and can initiate the subsequent chain of exothermic reactions. Fig. 5(a) plots $T_{critical}$ as a function of $E_{a_{sei}}$ showing, as expected, that $T_{critical}$ goes down as $E_{a_{sei}}$ goes down. Similarly, Fig. 5(b) plots $T_{critical}$ as a function of carbon content at anode (W_c) keeping all other parameters fixed. This plot shows that $T_{critical}$ increases as W_c goes down. This occurs because the larger the value of W_c, the more aggressive heat generation is, and therefore, thermal runaway occurs at lower temperatures. Both the above analyses are carried out for an oven test with oven temperature set to 160 °C, and considering all four decomposition reactions. Note that a distinction must be made here between between $T_{critical}$ and oven temperature. Although $T_{critical}$ is determined for a certain oven temperature, $T_{critical}$ is the temperature of the cell at which initiation of chain reaction occurs, which can be lower than the oven temperature. Such analyses demonstrate the capability of the theoretical model to predict the critical temperature for thermal runaway in a variety of complicated conditions that commonly occur in abuse testing of Li-ion cells as well as in real world applications.

The role of heat transfer processes, including conduction within the cell and convection on the outer surface in determining the onset of thermal runaway is examined next. Fig. 6 plots $T_{critical}$ as a function of the convective heat transfer coefficient h, for two different values of the radial thermal conductivity of the cell considering all four decomposition reactions that typically occur during thermal runaway. Fig. 6 shows that for low thermal conductivity of 0.15 W/m K, $T_{critical}$ rises with increase in h, but becomes stable beyond $h = 150$ W/m^2 K. However, for a high thermal conductivity cell, $T_{critical}$ continues to increase even for higher h values. This indicates that increasing the thermal conductivity of the cell helps increase the onset temperature of thermal runaway, making the cell inherently safer at higher temperatures. For a low thermal conductivity cell, increasing external convective cooling beyond a limit is not seen to delay thermal runaway.

Because the phenomena of thermal conduction within the cell and convection on the outer surface are closely coupled with each other, the simultaneous effect of both on $T_{critical}$ is examined. Fig. 7 presents a color plot of $T_{critical}$ as a function of h and k for heat generation kinetics corresponding to all four reactions. Curves corresponding to three values of $T_{critical}$ are also plotted. This figure shows that a low value of h, corresponding to natural convection cooling, leads to a $T_{critical}$ of 125 °C, even if the cell thermal conductivity is very poor. On the other hand, there is a lower limit of the value of k, below which a $T_{critical}$ of 145 °C or above is simply not possible, even with extremely aggressive thermal management, such as liquid cooling. At this $T_{critical}$ threshold, there is some benefit in improving the cell thermal conductivity. Increasing thermal conductivity reduces the required value of h, which might mean, for example, that inexpensive air cooling may replace the more complicated and expensive liquid cooling. This effect, however, saturates beyond a certain value of k. The $T_{critical} = 135$ °C curve exhibits intermediate behavior. It is interesting that even a relatively small

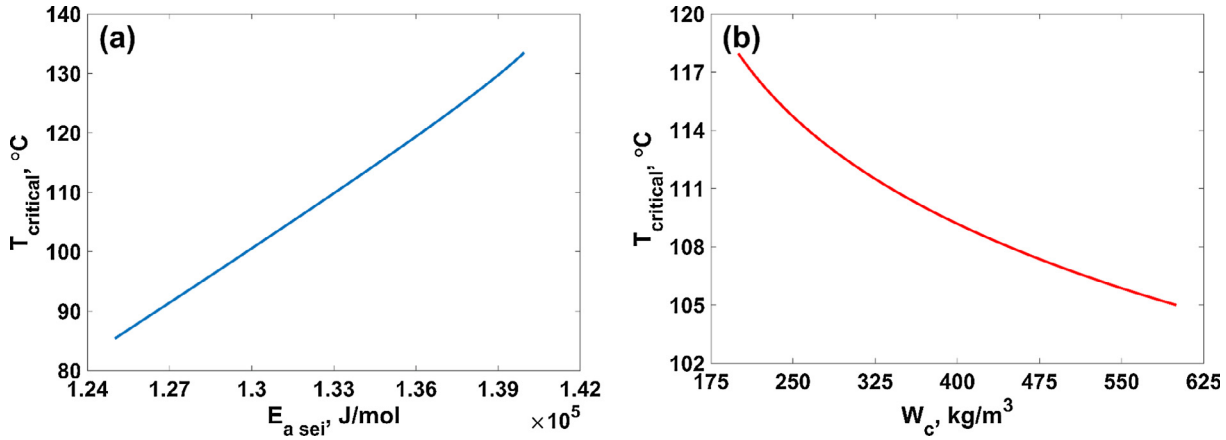

Fig. 5. Theoretically predicted variation of $T_{critical}$ considering all four key decomposition reactions in a Li-ion cell as a function of Arrhenius reaction kinetics parameters of the first reaction: (a) Variation with activation energy, $E_{a_{sei}}$, and (b) Variation with active material content, W_c.

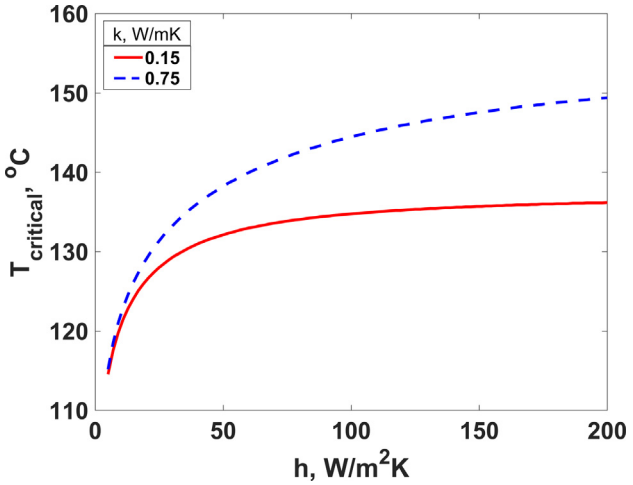

Fig. 6. Variation of $T_{critical}$ as a function of h for cells of two different thermal conductivities. In each case, the four key decomposition reactions relevant for thermal runaway in Li-ion cells are modeled.

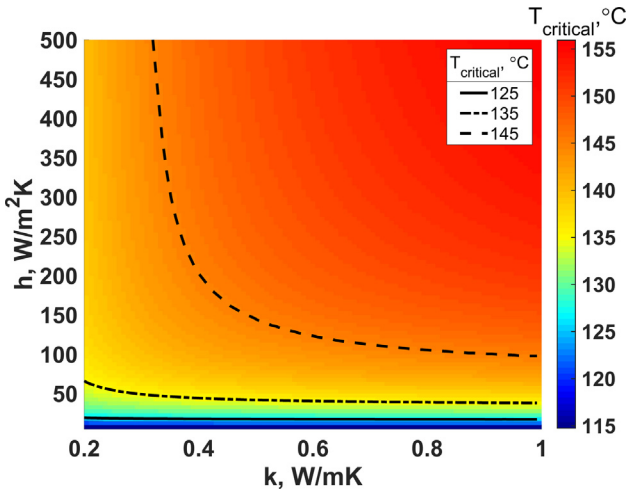

Fig. 7. Colorplot of $T_{critical}$ in the h-k parameter space based on the multiple reaction model with reactant consumption. Curves corresponding to three different values of $T_{critical}$ are also shown.

change of 10 °C in $T_{critical}$ within the curves shown dramatically changes the nature of the balance between thermal conduction and convective cooling. Fig. 7 contributes towards effective thermal design of Li-ion cells for thermal runaway prevention by quantifying these important trade-offs.

Oven tests are a common thermal abuse experiment to evaluate the safety of Li-ion cells. In a typical oven test, a Li-ion cell is placed in a high temperature oven to trigger the onset of thermal runaway in the cell. In general, the higher the oven temperature for onset of thermal runaway, the safer the cell is considered to be, as it allows the cell to be operated and stored safely at a higher temperature. Fig. 8 presents a colormap of *TRN* as a function of oven temperature and radial thermal conductivity of the cell. The black curve on the color plot corresponds to the value of 1.0. As seen from Fig. 8, an oven temperature of 160 °C results in *TRN* exceeding the threshold for the lowest thermal conductivity considered. Oven temperature of 160 °C or above is typical for causing onset of thermal runaway in commercially available cylindrical Li-ion cells [11,15]. With increase in thermal conductivity, the required oven temperature for *TRN* to exceed the critical threshold also increases. For a cell with thermal conductivity of 1.0 W/m K, for example, the oven temperature needs to be above 175 °C in order to cause thermal runaway. This shows that Li-ion cells with higher thermal conductivity may exhibit improved safety characteristics, making them safer to operate and store at temperatures higher than for lower thermal conductivity cells.

Finally, the *TRN* theoretical model for computing the value of $T_{critical}$ presented here is compared against $T_{critical}$ computations based on the theory presented by Frank-Kamenetskii in the context of self-ignition of

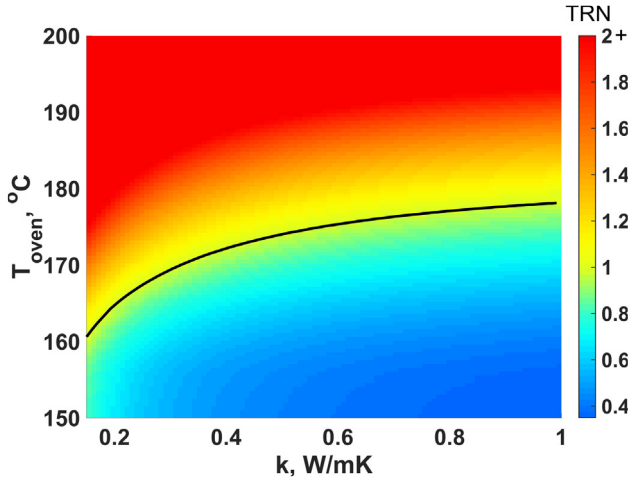

Fig. 8. Colorplot of *TRN* in the T_{oven}-k parameter space based on the multiple reaction model with reactant consumption. Curves corresponding to value of *TRN* = 1 are also shown.

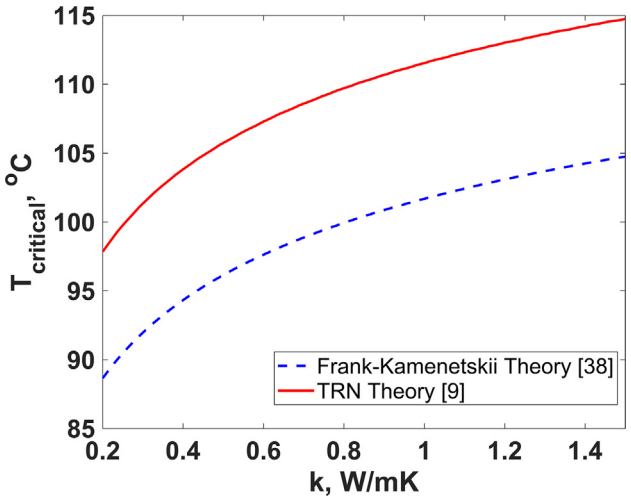

Fig. 9. Comparison of predicted value of $T_{critical}$ as a function of cell thermal conductivity, predicted from Thermal Runaway Number [9] and Frank-Kamenetskii [38] theories.

a combustible material [38]. Fig. 9 plots $T_{critical}$ as a function of cell thermal conductivity computed through both approaches. In this case, the convective heat transfer coefficient is assumed to be 500 $W/m^2 K$ and SEI decomposition reaction kinetics is assumed. This figure shows similar behavior of predictions from both theories. Both models predict an increase in $T_{critical}$ as k increases, and differ from each other only by a nearly-constant offset. In general, $T_{critical}$ for the *TRN* approach is greater than the Frank-Kamenetskii approach. Most likely, this is because the linearization process underlying Frank-Kamenetskii theory is more conservative than the *TRN* approach. Further, note that while the *TRN* approach exactly accounts for external cooling by imposing the appropriate convective boundary condition on the outer surface [9], Frank-Kamenetskii theory was originally derived for an isothermal outer surface [38] – which is not accurate in most realistic conditions – and corrections to account for a finite value of h derived later [47] involve approximations.

5. Conclusions

Thermal runaway is a serious concern that negatively affects the performance and safety of Li-ion based electrochemical energy conversion systems. Information about the maximum permissible temperature to avoid thermal runaway in such systems is critical for ensuring safety. This work contributes towards this goal by developing and experimentally validating a method for predicting the critical temperature. Experimental measurements in a variety of conditions are found to be in good agreement with predictions from the theoretical model. This work also highlights the key trade-offs between heat transfer within the cell and from the cell surface to the surroundings, both of which play a key role in the overall thermal balance of the cell. Careful consideration of such trade-offs is shown to result in useful insights into the thermal design of a Li-ion cell as well as its thermal ambient. In addition to improving the understanding of the fundamentals of heat transfer processes in a Li-ion cell, it is expected that results presented here may contribute towards the design of thermal management systems for improved safety of electrochemical energy conversion systems. For example, calculation of $T_{critical}$ based on the mathematical models presented here may be used for comparative study of thermal safety of a number of battery chemistries as well as the effect of various thermal management strategies. Information about the critical temperature can also be used for optimizing and improving thermal safety and performance of storage, transportation and real-time operation of Li-ion cells.

Acknowledgments

This material is based upon work supported by CAREER Award No. CBET-1554183 from the National Science Foundation.

References

[1] J.B. Goodenough, K.-S. Park, The Li-ion rechargeable battery: a perspective, J. Am. Chem. Soc. 135 (2013) 1167.
[2] B. Scrosati, J. Garche, Lithium batteries: status, prospects and future, J. Power Sources 195 (2010) 2419–2430.
[3] K. Shah, N. Balsara, S. Banerjee, M. Chintapalli, A.P. Cocco, W.K.S. Chiu, et al., State of the art and future research needs for multiscale analysis of Li-ion cells, J. Electrochem. Energy Conv. Storage 14 (2017) 020801.
[4] K. Shah, V. Vishwakarma, A. Jain, Measurement of multiscale thermal transport phenomena in Li-ion cells: a review, J. Electrochem. Energy Conv. Storage 13 (2016) 030801.
[5] T.M. Bandhauer, S. Garimella, T.F. Fuller, A critical review of thermal issues in lithium-ion batteries, J. Electrochem. Soc. 158 (2011) R1.
[6] M.N. Richard, J.R. Dahn, Accelerating rate calorimetry study on the thermal stability of lithium intercalated graphite in electrolyte. I. Experimental, J. Electrochem. Soc. 146 (1999) 2068.
[7] E.P. Roth, G. Nagasubramanian, Thermal stability of electrodes in Li-ion cells, Technical Report SAND2000-0345J Sandia National Laboratories, USA, 2000.
[8] P. Biensan, B. Simon, J.P. Peres, A. de Guibert, M. Broussely, J.M. Bodet, F. Perton, On safety of lithium-ion cells, J. Power Sources 82 (1999) 906–912.
[9] K. Shah, D. Chalise, A. Jain, Experimental and theoretical analysis of a method to predict thermal runaway in Li-ion cells, J. Power Sources 330 (2016) 167–174.
[10] R. Spotnitz, J. Franklin, Abuse behavior of high-power, lithium-ion cells, J. Power Sources 113 (2003) 81–100.
[11] T.D. Hatchard, D.D. MacNeil, A. Basu, J.R. Dahn, Thermal model of cylindrical and prismatic lithium-ion cells, J. Electrochem. Soc. 148 (2001) A755–A761.
[12] J. Jeevarajan, Safety of commercial lithium-ion cells and batteries, in: G. Pistoia (Ed.), Lithium-Ion Batteries, 2014, pp. 387–407.
[13] E.P. Roth, D.H. Doughty, D.L. Pile, Effects of separator breakdown on abuse response of 18650 Li-ion cells, J. Power Sources 174 (2007) 579–583.
[14] A.W. Golubkov, D. Fuchs, J. Wagner, H. Wiltsche, C. Stangl, G. Fauler, G. Voitic, A. Thaler, V. Hacker, Thermal-runaway experiments on consumer Li-ion batteries with metal-oxide and olivin-type cathodes, RSC Adv. 4 (2014) 3633–3642.
[15] C.F. Lopez, J.A. Jeevarajan, P.P. Mukherjee, Characterization of lithium-ion battery thermal abuse behavior using experimental and computational analysis, J. Electrochem. Soc. 162 (2015) A2163–2173.
[16] W. Cai, H. Wang, H. Maleki, J. Howard, E. Lara-Curzio, Experimental simulation of internal short circuit in Li-ion and Li-ion-polymer cells, J. Power Sources 196 (2011) 7779–7783.
[17] M.S. Wu, P.C.J. Chiang, J.C. Lin, Y.S. Jan, Correlation between electrochemical characteristics and thermal stability of advanced lithium-ion batteries in abuse tests – short-circuit tests, Electrochim. Acta 49 (2004) 1803–1812.
[18] S. Santhanagopalan, P. Ramadass, J.Z. Zhang, Analysis of internal short-circuit in a lithium ion cell, J. Power Sources 194 (2009) 550–557.
[19] T.D. Hatchard, S. Trussler, J.R. Dahn, Building a “smart nail” for penetration tests on Li-ion cells, J. Power Sources 247 (2014) 821–823.
[20] T. Yokoshima, D. Mukoyama, F. Maeda, T. Osaka, K. Takazawa, S. Egusa, S. Naoi, S. Ishikura, K. Yamamoto, Direct observation of internal state of thermal runaway in lithium ion battery during nail-penetration test, J. Power Sources 393 (2018) 67–74.
[21] A. Melcher, C. Ziebert, M. Rohde, H. Seifert, Modeling and simulation the thermal runaway behavior of cylindrical li-ion cells – computing of critical parameter, Energies 9 (2016) 292.
[22] D. Macneil, Z. Lu, Z. Chen, J. Dahn, A comparison of the electrode/electrolyte reaction at elevated temperatures for various Li-ion battery cathodes, J. Power Sources 108 (2002) 8–14.
[23] S. Drake, D. Wetz, J. Ostanek, S. Miller, J. Heinzel, A. Jain, Measurement of anisotropic thermophysical properties of cylindrical Li-ion cells, J. Power Sources 252 (2014) 298–304.
[24] J. Zhang, B. Wu, Z. Li, J. Huang, Simultaneous estimation of thermal parameters for large-format laminated lithium-ion batteries, J. Power Sources 259 (2014) 106–116.
[25] H. Maleki, S.A. Hallaj, J.R. Selman, R.B. Dinwiddie, H. Wang, Thermal properties of lithium-ion battery and components, J. Electrochem. Soc. 146 (1999) 947–954.
[26] V. Vishwakarma, A. Jain, Measurement of in-plane thermal conductivity and heat capacity of separator in Li-ion cells using a transient DC heating method, J. Power Sources 272 (2014) 378–385.
[27] J. Nanda, S.K. Martha, W.D. Porter, H. Wang, N.J. Dudney, M.D. Radin, D.J. Siegel, Thermophysical properties of $LiFePO_4$ cathodes with carbonized pitch coatings and organic binders: experiments and first-principles modeling, J. Power Sources 251 (2014) 8–13.
[28] V. Vishwakarma, C. Waghela, Z. Wei, R. Prasher, S.C. Nagpure, J. Li, F. Liu, C. Daniel, A. Jain, Heat transfer enhancement in a lithium-ion cell through improved material-level thermal transport, J. Power Sources 300 (2015) 123–131.
[29] A. Lazrak, J.F. Fourmigué, J.F. Robin, An innovative practical battery thermal management system based on phase change materials: numerical and experimental investigations, Appl. Therm. Eng. 128 (2018) 20–32.
[30] S.K. Mohammadian, Y.L. He, Y. Zhang, Internal cooling of a lithium-ion battery

using electrolyte as coolant through microchannels embedded inside the electrodes, J. Power Sources 293 (2015) 458–466.
[31] D. Anthony, D. Wong, D. Wetz, A. Jain, Improved thermal performance of a Li-ion cell through heat pipe insertion, J. Electrochem. Soc. 164 (2017) A961–967.
[32] Y. Ye, Y. Shi, L.H. Saw, A.A. Tay, Performance assessment and optimization of a heat pipe thermal management system for fast charging lithium ion battery packs, Int. J. Heat Mass Transf. 92 (2016) 893–903.
[33] L.H. Saw, Y. Ye, M.C. Yew, W.T. Chong, M.K. Yew, T.C. Ng, Computational fluid dynamics simulation on open cell aluminium foams for Li-ion battery cooling system, Appl. Energy 204 (2017) 1489–1499.
[34] Z. Rao, Z. Qian, Y. Kuang, Y. Li, Thermal performance of liquid cooling based thermal management system for cylindrical lithium-ion battery module with variable contact surface, Appl. Therm. Eng. 123 (2017) 1514–1522.
[35] Y. Lv, X. Yang, X. Li, G. Zhang, Z. Wang, C. Yang, Experimental study on a novel battery thermal management technology based on low density polyethylene-enhanced composite phase change materials coupled with low fins, Appl. Energy 178 (2016) 376–382.
[36] W. Wu, X. Yang, G. Zhang, X. Ke, Z. Wang, W. Situ, et al., An experimental study of thermal management system using copper mesh-enhanced composite phase change materials for power battery pack, Energy 113 (2016) 909–916.
[37] W. Wu, X. Yang, G. Zhang, K. Chen, S. Wang, Experimental investigation of the thermal performance of heat pipe-assisted phase change material based battery thermal management system, Appl. Therm. Eng. 141 (2018) 1092–1100.
[38] D.A. Frank-Kamenetskii, Diffusion and Heat Transfer in Chemical Kinetics, second ed., Plenum Press, New York, 1969.
[39] S. Wilke, B. Schweitzer, S. Khateeb, S. Al-Hallaj, Preventing thermal runaway propagation in lithium ion battery packs using a phase change composite material: an experimental study, J. Power Sources 340 (2017) 51–59.
[40] A. Hofmann, N. Uhlmann, C. Ziebert, O. Wiegand, A. Schmidt, T. Hanemann, Preventing Li-ion cell explosion during thermal runaway with reduced pressure, Appl. Therm. Eng. 124 (2017) 539–544.
[41] N. Özişik, Heat Conduction, second ed., John Wiley & Sons, 1993.
[42] F.P. Incropera, D.P. Dewitt, Introduction to Heat Transfer, third ed., Wiley Inc., 2006.
[43] B. Ayyub, R.H. McCuen, Numerical Analysis for Engineers: Methods and Applications, second ed., CRC Press, 2015.
[44] D. Anthony, D. Sarkar, A. Jain, Non-invasive, transient determination of the core temperature of a heat-generating solid body, Sci. Rep. 6 (35886) (2016) 1–10.
[45] K. Shah, C. McKee, D. Chalise, A. Jain, Experimental and numerical investigation of core cooling of Li-ion cells using heat pipes, Energy 113 (2016) 852–860.
[46] M. Parhizi, M.B. Ahmed, A. Jain, Determination of the core temperature of a Li-ion cell during thermal runaway, J. Power Sources 370 (2017) 27–35.
[47] P.F. Beever, Self-heating and spontaneous combustion, in: P.J. DiNenno (Ed.), SFPE Handbook of Fire Protection Engineering, first ed., National Fire Protection Association, Quincy, MA, 1988.